Assessment of the role of hydrogen to produce high-temperature heat in the steel industry

Journal of Cleaner Production 388 (2023) 135969

Contents lists available at ScienceDirect

Journal of Cleaner Production

journal homepage: www.elsevier.com/locate/jclepro

Assessment of the role of hydrogen to produce high-temperature heat in the steel industry

Paolo Marocco, Marta Gandiglio *, Davide Audisio, Massimo Santarelli

Department of Energy, Politecnico di Torino, Corso Duca degli Abruzzi 24, 10129, Torino, Italy

ARTICLE INFO

Handling Editor: Kathleen Aviso

Keywords:
Hydrogen
Electrolysis
Steel industry
Decarbonisation
Optimal design
CO_2 emission

ABSTRACT

The iron and steel industry is a major source of industrial greenhouse gas emissions, accounting for 7–9% of global energy-related CO_2 emissions. Current steel production routes are therefore expected to undergo a profound decarbonisation process in the coming decades.

This work aims to shed light on the role of hydrogen in decarbonising the supply of high-temperature heat in the steel sector by means of an optimisation framework. The model includes on-site hydrogen production using a low-temperature electrolyser integrated with a compression and storage system and gas burners, which can be fed with hydrogen and/or natural gas to cover the process heat demand. The assessment also takes advantage of real thermal load profiles of a scrap-based electric arc furnace steel plant.

A sensitivity analysis is conducted on the electricity, natural gas and carbon prices. Cost-optimal maps are then derived to unveil the combination of energy and carbon prices at which hydrogen becomes convenient for heat production in the steel industry. A general relationship to define the cost-effectiveness of hydrogen is also given.

The results show that, at current carbon prices (about 100 €/t_{CO2}), the use of hydrogen becomes economically convenient when the electricity price is less than 0.4–0.6 times the natural gas price. In scenarios with electricity prices lower than about 0.10 €/kWh, as could occur with on-site renewable electricity generation, hydrogen cost falls below 6.5 €/kg_{H2}, leading to cost savings of up to 60–70% compared to a natural gas-based configuration. Finally, when total CO_2 emissions (direct + indirect) are considered, hydrogen becomes environmentally beneficial if the electricity carbon intensity is below 123 g_{CO2}/kWh.

1. Introduction

Global greenhouse gas emissions reached their highest level ever in 2021 (40.8 Gt CO_2 equivalent). Of these emissions, 89% are due to energy combustion and industrial processes (IEA, 2021). The iron and steel sector, which produces core materials for today's society and whose demand is expected to increase in the coming decades, is one of the largest emitters of carbon dioxide (Hoffmann et al., 2020). It was responsible for 845 Mtoe of global energy consumption in 2019 (IEA, 2020), representing 20% of industrial energy use and 8% of total final energy consumption (Kurrer, 2020; Fan and Friedmann, 2021). This makes the iron and steel sector the second largest energy consumer after the chemical industry and responsible for about 7–9% of global energy-related CO_2 emissions (Spreitzer and Schenk, 2019).

Steel production is currently dominated by the Blast Furnace – Basic Oxygen Furnace (BF-BOF) route, which accounts for 71% of global steel demand. It is followed by secondary steelmaking (employing steel scrap), which accounts for 24% of the market and employs a scrap-based Electric Arc Furnace (EAF). Finally, the innovative electrical-driven Direct Reduced Iron – Electric Arc Furnace (DRI-EAF) process covers about 5% of total demand. According to the World Steel Association, the production of 1 tonne of steel emits on average 1.85 tonnes of CO_2 (Hoffmann et al., 2020). Furthermore, the steel sector is part of the European Emission Trading System (ETS) and is subject to penalties for emitted CO_2. A sharp increase in the carbon price under the ETS market was observed in early 2022, with peaks close to 100 €/t of CO_2 (EUROFER (European Steel Association), 2022).

As a result, the steel sector has begun to focus on the possible introduction of low-carbon fuels such as hydrogen (H_2), which can reduce fossil fuel consumption and associated carbon emissions during the production process. Hydrogen has indeed been mentioned as one of the pillars for the decarbonisation of the steel sector, along with carbon capture and carbon-neutral biomass (Fan and Friedmann, 2021). In steel production, hydrogen can be used as a primary reducing agent in the

* Corresponding author.
E-mail address: marta.gandiglio@polito.it (M. Gandiglio).

https://doi.org/10.1016/j.jclepro.2023.135969
Received 7 November 2022; Received in revised form 23 December 2022; Accepted 7 January 2023
Available online 9 January 2023

DRI process, as a secondary reducing agent in the BF-BOF process and – in both routes – as a fuel for the generation of high-temperature heat (IRENA, 2022). When hydrogen is used as a substitute for natural gas (NG), syngas or coke in steel production, some adjustments to the existing equipment (burners and furnaces) are required to cope with the differences in terms of calorific value, density, flame temperature and flame propagation speed (E&M Combustion, 2020).

As can be seen from the review articles by Liu et al. (2021) and Wang et al. (2021), the feasibility studies and techno-economic analyses available in the literature mostly focus on the integration of hydrogen in the steel industry as a reducing agent. Rechberger et al. (2020) compared the NG-based and hydrogen-based DRI processes. They showed that the hydrogen-based route can offer enormous potential for green steelmaking, although this depends heavily on the carbon footprint of the electricity used for hydrogen production. More specifically, when indirect emissions are considered, the CO_2 emissions of the H_2-based process are lower than those of the NG-based process only if the grid carbon intensity is less than ~120 g_{CO2}/kWh. Vogl et al. (2018) investigated the use of hydrogen in the DRI process and showed that hydrogen direct reduction becomes cost competitive at a carbon price of 34–68 €/t and electricity cost of 40 €/MWh. The electrical demand to produce steel by direct reduction with hydrogen was estimated at 3.48 MWh per tonne of liquid steel, mainly due to the consumption of the electrolyser. Fan and Friedmann (2021) reported that the conversion of DRI-EAF plants from natural gas to green hydrogen causes a cost increase of more than 400 € per tonne of hot metal produced. They also showed that, if green hydrogen is employed in BF-BOF, the cost increase is about 200 € per tonne of hot metal. Moreover, if blue hydrogen is used, the cost increase can be reduced by more than 50% in both cases (i.e. DRI-EAF and BF-BOF).

The studies mentioned above investigated the techno-economic feasibility of introducing hydrogen as a reducing agent in steel production. However, to achieve complete decarbonisation of the steel industry, the use of hydrogen as a heating fuel in furnaces could also be considered. The iron and steel industry, together with the cement and chemical sectors, is responsible for 85% of the world's industrial heat demand, and 95% of this heat is currently generated from fossil sources (IEA, 2019). Almost all process heat demand in steelmaking occurs at very high temperatures (>500 °C), with values up to 1350 °C in furnaces for rolling and forging. Electrification of high-grade heat, even if technically feasible, entails the redesign of industrial equipment, which results in high capital expenditures. In contrast, using hydrogen in existing burners requires partial redesign, making it a preferred and less invasive solution for decarbonising high-temperature heat (IRENA, 2022). There are different works in the literature that examine the effects of adding hydrogen to natural gas in existing industrial furnaces. Leicher et al. (2018) discussed how hydrogen mixed with natural gas can affect industrial end-users and found that hydrogen can have an impact on the burner performance in terms of heat transfer, efficiency, flame shape and NO_x emissions. However, these effects can be mitigated by advanced measurement and control technologies. By properly adjusting the firing rate and the excess air ratio, no significant increase in NO_x emissions or loss of efficiency was observed at a hydrogen content of 50% by volume. Mayrhofer et al. (2021) investigated the use of NG-hydrogen mixtures as an alternative fuel for industrial heat treatment furnaces. The authors evaluated two control systems in terms of their ability to regulate the gas flow rate at different hydrogen contents, with the aim of analysing the capability to retrofit existing furnaces. It was found that an electric compound control system is more suitable for applications with variable hydrogen content, even though it incurs higher costs compared to the pneumatic control variant.

The literature also includes high-level scenario analyses, such as that of Karakaya et al. (2018), which examined the possible pathways for a sustainable transition in the Swedish iron and steel industry. The positive experience of green steel production in Sweden was also explored by Öhman et al. (2022), who investigated the conditions for transferring a particular green steel production process (hydrogen-reduced sponge iron) from Sweden to other primary steel producing countries in Europe. They stressed that, in order to promote hydrogen-based steelmaking in Europe, it is necessary that energy and industry transitions are aligned, including the creation of a supportive policy framework. A complete picture of existing projects and initiatives worldwide to decarbonise the steel industry was developed by Zhang et al. (2021). The authors examined the different pathways to green steel production and found that hydrogen has great potential in the metallurgic industry: from the DRI process to its use as a reducing agent to renovate existing blast furnaces, but also in innovative early-stage applications such as the flash smelting method. Japan, the USA and China are among the leading countries in initiatives to decarbonise the steel industry and are also leading players in the development of green hydrogen technologies, as shown in (Ampah et al., 2022).

Although decarbonisation of steel production is widely explored in the literature, there are no studies that address the optimal design of energy systems for industrial heat supply in furnaces. The present work seeks to fill this gap by developing an optimisation framework that is capable to compute the cost-optimal solution for the coverage of the process heat demand of a steel plant. Both hydrogen, produced on-site by water electrolysis, and natural gas from the grid were considered as fuels for the generation of heat. A sensitivity analysis on the energy prices (electricity and natural gas) and carbon price was carried out to provide a comprehensive overview about the cost-effectiveness of hydrogen use for heat generation. To this end, a mixed-integer linear programming (MILP) model was formulated to handle both design and scheduling of the energy system. A piecewise affine (PWA) approximation of the electrolyser efficiency curve was also included for an accurate modelling of the part-load performance of the electrolyser. The analysis takes advantage of real thermal demand profiles of a scrap-based EAF steel plant located in northern Italy.

This work is structured as follows: Section 2 describes the MILP-based optimisation framework including the modelling of the system components and the definition of the objective function. The case study is presented in Section 3, while the main techno-economic assumptions are reported in Section 4. The results are presented and discussed in Section 5 and finally the main conclusions of this analysis are summarised in Section 6.

2. Methodology

The layout of the energy system is shown in Fig. 1. It includes the following components: an electrolyser to produce hydrogen, a hydrogen compressor, a pressurised hydrogen tank, and gas burners to cover the process heat demand of the steel plant. The electrical power required is drawn from the electrical grid, while the natural gas is taken from the gas grid. The hydrogen produced by the electrolyser can be fed directly to the gas burners or stored in the pressurised tank. The gas mixture feeding the burners consists of natural gas and/or hydrogen. The nodes of the energy system – where power balances take place – are also shown in Fig. 1 (they are denoted by N_i).

An MILP model was developed to identify the optimal size and operation for all components of the energy system to meet the thermal demand of the steel plant with the minimum net present cost (NPC). The overall structure of the MILP-based optimisation framework is shown in Fig. 2. An hourly time-step resolution (t) and a time horizon (T) of one year were considered in this analysis.

The input parameters of the optimisation model are the following:

- The thermal demand $\forall\, t \in T$
- The prices of electricity and natural gas $\forall\, t \in T$
- The carbon price and the prices of the utilities involved in the energy system (water, oxygen)

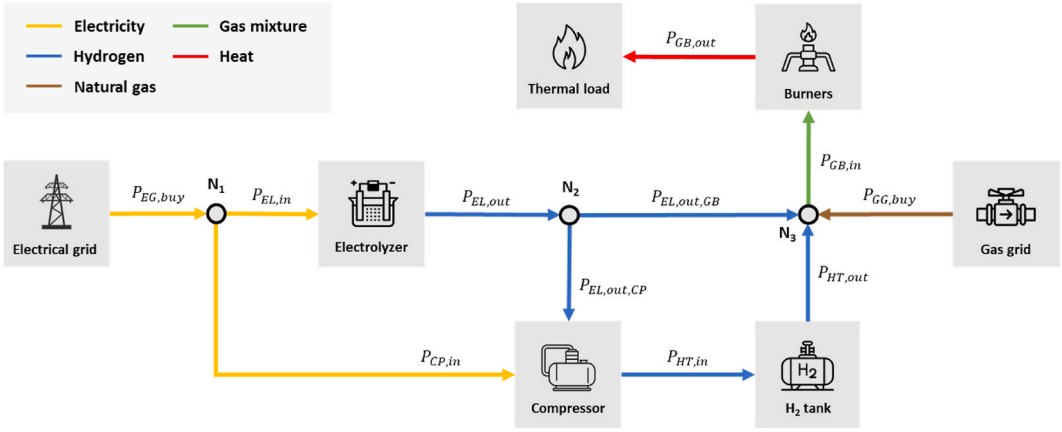

Fig. 1. Layout of the energy system model.

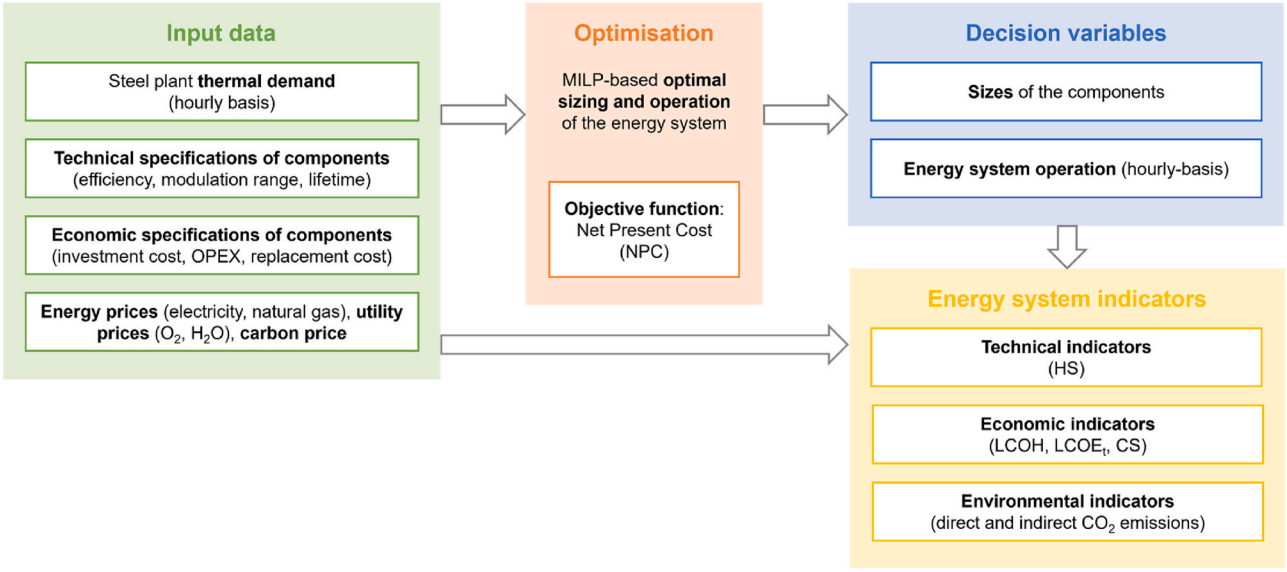

Fig. 2. Optimisation framework for the optimal design of the energy system.

- Techno-economic data of the different components of the energy system, i.e. electrolyser (EL), hydrogen compressor (CP), hydrogen tank (HT) and gas burner (GB).

Both design (i.e. sizes) and operation variables are computed by the optimisation problem. Specifically, the following decision variables are returned:

- The sizes of all components of the energy system, i.e. EL, CP, HT, GB
- The input power (gas) to the GB, i.e. natural gas from the gas grid and hydrogen from the storage tank or directly from the electrolyser, $\forall\, t \in T$
- The electrical power drawn from the electrical grid, i.e. the input power (electricity) to the EL and CP, $\forall\, t \in T$
- The output power from the GB (heat) and the EL (hydrogen) $\forall\, t \in T$
- The charging and discharging power (hydrogen) of the HT $\forall\, t \in T$
- The amount of energy (hydrogen) stored in the HT $\forall\, t \in T$.

As shown in Fig. 2, based on the optimisation run, specific techno-economic and environmental indicators have been computed for an in-depth comparison of the different scenarios.

The optimisation problem was formulated in the MATLAB environment and solved using the commercial software IBM CPLEX (IBM, 2022).

The main relationships required to model the energy system and compute the objective function are presented below. Instead, the thermal demand profile and all techno-economic data assumed in this analysis are described in detail in Section 3 and Section 4, respectively.

2.1. Power balances

In each time interval t of the simulation, three main power balances must be satisfied. The first power balance, denoted by N_1 in Fig. 1, is defined as follows:

$$P_{EG,buy}(t) = P_{EL,in}(t) + P_{CP,in}(t) \quad (1)$$

where $P_{EG,buy}$ is the power taken from the electrical grid, $P_{EL,in}$ is the power requested by the electrolyser and $P_{CP,in}$ is the power consumed by the compressor to pressurise the hydrogen stream that is sent to the storage tank.

The second power balance refers to node N_2 and is expressed by the following relationship:

$$P_{EL,out}(t) = P_{EL,out,GB}(t) + P_{EL,out,CP}(t) \quad (2)$$

where $P_{EL,out}$ is the total amount of hydrogen produced by the electrolyser, which can be sent directly to the burner ($P_{EL,out,GB}$) or to the compressor to be stored in a tank ($P_{EL,out,CP}$).

The third power balance, i.e. node N_3, is reported as follows:

$$P_{GB,in}(t) = P_{GG,buy}(t) + P_{EL,out,GB}(t) + P_{HT,out}(t) \quad (3)$$

As shown in the above equation, the inlet power to the gas burner ($P_{GB,in}$) is given by the natural gas bought from the gas grid ($P_{GG,buy}$) and/or hydrogen. The hydrogen can be taken directly from the electrolyser ($P_{EL,out,GB}$) or from the pressurised tank ($P_{HT,out}$).

All power values related to fuel streams are given on a lower heating value (LHV) basis.

2.2. Modelling of components

The sizes of the components involved in the energy system are treated as continuous variables. They are constrained to a minimum value and a maximum value, according to the following relationships:

$$P_{i,rated,min} \leq P_{i,rated} \leq P_{i,rated,max} \quad (4)$$

$$E_{j,rated,min} \leq E_{j,rated} \leq E_{j,rated,max} \quad (5)$$

where $P_{i,rated}$ (in kW) corresponds to the rated power of the i-th component (with i = EL, CP, GB) and $E_{j,rated}$ (in kWh) represents the rated capacity of the j-th storage component (with j = HT). The rated power refers to the rated electrical power consumption for EL and CP and to the rated thermal power production for GB. The minimum value of Eqs. (4) and (5) was set to zero, which means that a certain component is selected whenever the MILP-based optimisation returns a value for its size greater than zero.

2.2.1. Electrolyser

Eq. (6) imposes the constraints on the minimum and maximum operating power of the electrolyser:

$$y_{EL,min} \cdot P_{EL,rated,aux}(t) \leq P_{EL,in}(t) \leq y_{EL,max} \cdot P_{EL,rated,aux}(t) \quad (6)$$

The terms $y_{EL,min}$ and $y_{EL,max}$ are the lower and upper limits of the electrolyser modulation range. $P_{EL,in}$ (in kW) is the inlet power to the electrolyser (in terms of electrical power), whereas $P_{EL,rated,aux}$ (in kW) is an auxiliary variable used to model the on-off status of the electrolyser system and define its operating range. It is expressed according to the following equation:

$$P_{EL,rated,aux}(t) = P_{EL,rated} \cdot \delta_{EL}(t) \quad (7)$$

where $P_{EL,rated}$ (in kW) is the rated power of the electrolyser and δ_{EL} is a binary variable that is equal to 1 when electrolyser is on or 0 when off. The introduction of $P_{EL,rated,aux}$ is necessary to treat the product of $P_{EL,rated}$ and δ_{EL} (which are both decision variables) as a set of linear inequalities, as described by Marocco et al. (2022).

A part-load performance curve was also included in the MILP-based model to have a more accurate assessment of the electrolyser operation. The EL performance curve, which relates the outlet hydrogen power to the inlet electrical power, was implemented within the MILP framework by means of a PWA approximation. Following the procedure explained in (Marocco et al., 2021a), the performance curve was divided into p linear segments that approximate the curve. The following constraint was then applied for each i-th line segment of the curve, $i \in \{1, \ldots, p\}$:

$$P_{EL,out}(t) \leq \alpha_{EL,i} \cdot P_{EL,in}(t) + c_{\beta,EL,i} \cdot P_{EL,rated,aux}(t) \quad (8)$$

where $P_{EL,in}$ and $P_{EL,out}$ (in kW) are the inlet (electricity) and outlet (hydrogen) power of the electrolyser, while $\alpha_{EL,i}$ and $c_{\beta,EL,i}$ are the coefficients of the i-th line segment.

2.2.2. Hydrogen compressor

The electrical power consumed by the hydrogen compressor ($P_{CP,in}$, in kW) was computed as follows:

$$P_{CP,in}(t) = \frac{P_{EL,out,CP}(t) \cdot l_{CP}}{LHV_{H_2}} \quad (9)$$

where $P_{EL,out,CP}$ (in kW) is the hydrogen power coming from the electrolyser and going to the compressor, l_{CP} (in MJ/kg) is the specific consumption of the compressor, and LHV_{H_2} (in MJ/kg) is the lower heating value of hydrogen.

Eq. (10) was added to ensure that the hydrogen sent to the compressor ($P_{EL,out,CP}$, in kW) is equal to the hydrogen at the inlet of the storage tank ($P_{HT,in}$, in kW).

$$P_{EL,out,CP}(t) = P_{HT,in}(t) \quad (10)$$

Analogously to the modelling of the electrolyser component (see Eq. (6)), linear constraints were introduced to describe the operating range of the compressor.

2.2.3. Hydrogen tank

The pressurised tank is used to store the excess hydrogen from the electrolyser. At each time step, the energy in the storage system (E_{HT}, in kWh) can be defined as:

$$E_{HT}(t+1) = E_{HT}(t) + P_{HT,in}(t) \cdot \Delta t - P_{HT,out}(t) \cdot \Delta t \quad (11)$$

where Δt is the time step, $P_{HT,in}$ is the input power to the tank (in terms of hydrogen) and $P_{HT,out}$ is the output power from the tank (in terms of hydrogen). A boundary condition was set for the first time step of the simulation:

$$E_{HT}(t_{in}) = E_{HT,rated} \cdot LOH_{in} \quad (12)$$

where LOH_{in} corresponds to the level of hydrogen (LOH) of the storage at the beginning of the simulation and $E_{HT,rated}$ (in kWh) is the rated capacity of the hydrogen tank. A storage autonomy constraint was also added to guarantee that the energy stored at the beginning of the year (t_{in}) is equal to that at the end of the year (t_{end}), as described by the equation below:

$$E_{HT}(t_{end}) = E_{HT}(t_{in}) \quad (13)$$

Finally, the following inequality constraints are required to limit the energy that can be stored in the HT:

$$E_{HT}(t) \leq E_{HT,rated} \cdot LOH_{max} \quad (14)$$

$$E_{HT}(t) \geq E_{HT,rated} \cdot LOH_{min} \quad (15)$$

where LOH_{min} and LOH_{max} are the minimum and maximum LOH values of the hydrogen tank. The LOH is the ratio between the stored energy and the rated capacity of the hydrogen storage tank.

2.2.4. Gas burner

It was assumed that the process heat demand is covered by a single gas burner. The gas burner operating range was modelled through Eq. (6), adapted for the GB component. The thermal power generated at the GB outlet ($P_{GB,out}$, in kW) was computed as follows:

$$P_{GB,out}(t) = P_{GB,in}(t) \cdot \eta_{GB} \quad (16)$$

where $P_{GB,in}$ is defined in Eq. (3) and η_{GB} is the GB efficiency.

2.3. Objective function

The objective function of the optimisation problem is the net present cost (NPC) of the energy system, i.e. the sum of all costs associated with the energy system throughout its lifetime. It is defined as the sum of the

capital expenditure of the plant ($C_{NPC,capex,tot}$) and the net operating expenditure ($C_{NPC,opex,tot}$):

$$C_{NPC,tot} = C_{NPC,capex,tot} + C_{NPC,opex,tot} \quad (17)$$

As shown in Eq. (18), the $C_{NPC,capex,tot}$ term, which occurs at the beginning of the analysis period, is equal to the sum of the capital expenditures for all components involved in the energy system, i.e. EL, CP and HT. The gas burner is already present in the steel plant and for this reason its investment cost was not included in the economic evaluation. Moreover, the cost of converting the GB from natural gas to hydrogen can be considered negligible with respect to the total NPC, as explained in Section 4.

$$C_{NPC,capex,tot} = C_{capex,EL} + C_{capex,CP} + C_{capex,HT} \quad (18)$$

The net operating expenditure ($C_{NPC,opex,tot}$) was evaluated as follows:

$$C_{NPC,opex,tot} = \sum_{n=1}^{N} \frac{C_{opex,tot}}{(1+d)^n} \quad (19)$$

Where n is a certain year over the lifetime of the plant (N), d is the discount rate and $C_{opex,tot}$ (in €) is the annual net operating expenditure of the energy system. The latter term includes the following contributions:

- The annual operating costs for each i-th component (including the replacement costs), $C_{opex,i}$
- The annual cost of electricity purchased from the electrical grid to feed the EL and CP, $C_{EG,buy}$
- The annual cost of natural gas purchased from the gas grid to feed the GB, $C_{GG,buy}$
- The annual cost of water purchased to feed the EL, $C_{H_2O,buy}$
- The annual cost associated with the CO_2 emissions, C_{CO_2}
- The annual revenue from the sale (or self-consumption) of oxygen produced as a by-product of the electrolyser operation, $C_{O_2,sell}$.

The $C_{opex,tot}$ term can therefore be computed as (with i = EL, CP, HT, GB):

$$C_{opex,tot} = \sum_i (C_{opex,i}) + C_{EG,buy} + C_{GG,buy} + C_{H_2O,buy} + C_{CO_2} - C_{O_2,sell} \quad (20)$$

The annual energy costs ($C_{EG,buy}$ and $C_{GG,buy}$) were obtained by multiplying the energy purchased from the grid (electricity and natural gas, in kWh) by the prices of electricity and natural gas (expressed in €/kWh). The annual cost associated with CO_2 emissions (C_{CO_2}) was computed as the annual direct CO_2 emissions (first term of Eq. (25)) multiplied by the carbon price taken from the European ETS market. The annual oxygen revenue ($C_{O_2,sell}$) was assessed as the oxygen produced annually (in kg) multiplied by the specific price the steel plant pays for oxygen currently purchased from an external supplier (in €/kg).

2.4. Energy system indicators

As shown in Fig. 2, a set of indicators has been calculated after the optimisation process.

2.4.1. Technical indicators

Based on the optimal operation of the energy system throughout the year, the hydrogen share (HS) was determined. It corresponds to the annual fraction of the thermal load covered by hydrogen and was evaluated according to the following equation:

$$HS = \sum_{t=1}^{8760} \frac{P_{EL,out,GB}(t) + P_{HT,out}(t)}{P_{GB,in}(t)} \quad (21)$$

In some scenarios, the HS was set as a constraint in the definition of the optimisation problem.

2.4.2. Economic indicators

The levelised cost of thermal energy ($LCOE_t$) and the levelised cost of hydrogen (LCOH) were used to compare the different scenarios from an economic perspective. The $LCOE_t$ (in €/kWh) was defined by the following relationship:

$$LCOE_t = \frac{C_{NPC,tot}}{\sum_{n=1}^{N} E_t \cdot (1+d)^{-n}} \quad (22)$$

where E_t (in kWh) is the annual demand of thermal energy of the steel plant. The LCOH (in €/kg) was instead assessed as:

$$LCOH = \frac{C_{NPC,H_2}}{\sum_{n=1}^{N} M_{H_2} \cdot (1+d)^{-n}} \quad (23)$$

where M_{H_2} (in kg) is the total amount of hydrogen produced annually and C_{NPC,H_2} is the NPC of the hydrogen system (production and storage) over the project lifetime. This means that OPEX related to the gas burner, costs of natural gas purchased from the grid and costs due to CO_2 emissions are not considered in the C_{NPC,H_2} term.

The cost saving (CS) indicator was also defined to estimate the economic saving (in percentage) between the optimal solution and the configuration with only NG. It was computed as follows:

$$CS = \frac{C_{NPC,tot} - C_{NPC,tot,NG}}{C_{NPC,tot,NG}} \quad (24)$$

where $C_{NPC,tot}$ is the NPC of the optimal solution and $C_{NPC,tot,NG}$ is the NPC of the scenario in which only NG is fed to the burner (i.e. HS equal to zero).

2.4.3. Environmental indicators

An environmental assessment was also carried out estimating the direct and indirect (Scope 1 and 2) CO_2 emissions of the steel plant. The annual total CO_2 emissions ($m_{CO_2,yr}$, in kt/yr) can be derived as:

$$m_{CO_2,yr} = \sum_{t=1}^{8760} \left(EF_{GB} \cdot P_{GG,buy} + ECI \cdot P_{EG,buy}\right) \cdot 10^{-9} \quad (25)$$

The first term in equation (25) refers to the direct emissions and depends on the natural gas drawn from the gas grid ($P_{GG,buy}$, in kW) and on the emissions factor of the gas burner (EF_{GB}, in g_{CO2}/kWh). The second term is related to the indirect emissions and is evaluated as the electricity carbon intensity (ECI, in g_{CO2}/kWh) multiplied by the electricity purchased from the grid ($P_{EG,buy}$, in kW).

The calculation of the direct emissions is based on the assumption that the natural gas taken from the grid is 100% methane (CH_4) and that all the carbon contained in the fuel is converted into CO_2. The emission factor of the gas burner (EF_{GB}, in g_{CO2}/kWh) can thus be expressed as follows:

$$EF_{GB} = \frac{MW_{CO_2} \cdot 3600}{LHV_{CH_4} \cdot MW_{CH_4}} \quad (26)$$

where LHV_{CH_4} (in MJ/kg) is the lower heating value of methane, and MW_{CO_2} and MW_{CH_4} (in g/mol) are the molecular weights of carbon dioxide and methane, respectively. As previously reported, an economic cost is also associated with the direct CO_2 emissions (in the framework of the European ETS market).

3. Case study

The methodology was applied to the case study of a scrap-based EAF steel plant in northern Italy. The steel melting section is the first step of the whole process and the most energy intensive. It consumes most of the electricity and a significant amount of natural gas. The ingots, billets,

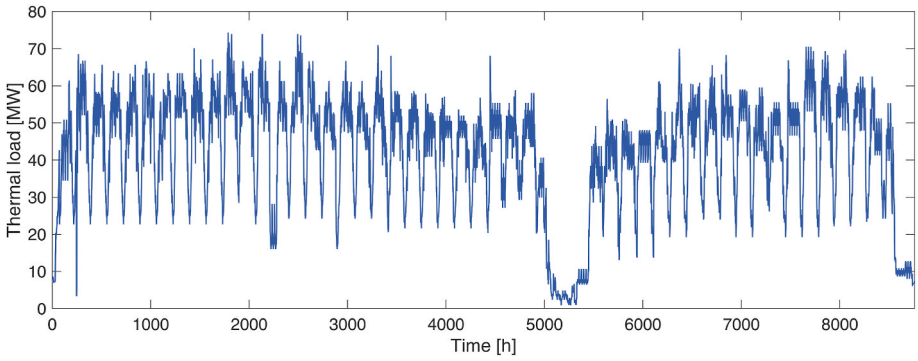

Fig. 3. Process heat demand of the steel plant.

bars and blooms produced are then sent to the other departments for the rolling process, thermal and chemical treatment and finishing. In all these steps there are several NG-fuelled furnaces, which are responsible for a large part of the CO_2 emissions. The overall process heat demand was evaluated as the sum of the thermal load of all 70 burners available in the plant (about 370 GWh/year). In the model, it is considered a single reference burner that can be fed with natural gas, hydrogen or a mixture of the two gases.

Fig. 3 shows the process heat demand of the steel plant with an hourly time resolution. It refers to the year 2019, but the trend is representative of a typical year for the steel plant. It shows a weekly variation (weekdays/weekends) with an average value of 42.2 MW and some peaks above 70 MW (maximum value of 74.3 MW). The lowest value is 0.96 MW and occurs in summer when the steel plant operation is restricted.

Table 1
Techno-economic assumptions.

Parameter	Unit	Value
Electrolyser		
Efficiency	%	Efficiency curve
Operating range	% (of rated power)	10–100
Operating pressure	bar	30
Stack lifetime	yr	10
BOP lifetime	yr	20
CAPEX	€/kW_{el}	1188
OPEX – fixed (annual)	€/kW_{el}	15.84
OPEX – variable (annual)	€/kWh_{el}	0.04
Installation cost	%CAPEX	10
Stack replacement cost	%CAPEX	35
Hydrogen compressor		
Specific consumption	MJ/kg_{H2}	4
Operating range	% (of rated power)	0–100
Lifetime	yr	20
CAPEX	€/kW_{el}	1600
OPEX (annual)	%CAPEX	2
Installation cost	%CAPEX	10
Hydrogen tank		
Maximum pressure	bar	200
Lifetime	yr	20
CAPEX	€/kg_{H2}	470
OPEX (annual)	%CAPEX	2
Installation cost	%CAPEX	10
Gas burners		
Efficiency	%	98
Operating range	% (of rated power)	0–100
CAPEX	€/kW_{th}	63.32
OPEX (annual)	%CAPEX	3
Energy, CO_2 and utility prices		
Electricity (Ref. scenario)	€/kWh_{el}	0.18
Natural gas (Ref. scenario)	€/kWh_{NG}	0.08
Carbon (Ref. scenario)	€/t_{CO2}	85
Water	€/kg_{H2}	0.08
Oxygen	€/kg_{O2}	0.05
Other assumptions		
Discount rate	%	4
Lifetime of the plant	yr	20

4. Techno-economic assumptions

The techno-economic data for the analysis are given in Table 1. A proton exchange membrane (PEM) electrolyser was considered for hydrogen production. The efficiency curve of the PEM electrolyser, shown in Fig. 4, was taken from (Zauner et al., 2019). It was implemented within the MILP-based optimisation framework according to the PWA approximation described in Section 2.2.1. As can be seen in Fig. 4, the electrolyser efficiency is 55% at rated power, while the peak efficiency is 65% and occurs at 20% of the rated power. The electrolyser operates with a modulation range of 10–100% (percent of the rated power) (Marocco et al., 2021a). The lower limit was set to ensure that the electrolyser operates efficiently and safely. Low partial loads would indeed lead to safety problems (due to hydrogen cross-diffusion) and lower efficiency (due to energy consumption by auxiliary components) (Marocco et al., 2021b). The specific investment cost of the PEM electrolyser was assumed to be 1188 €/kW (Böhm et al., 2020), which is representative of the cost of MW-scale electrolysers in the current market (Böhm et al., 2020; Proost, 2019). The operating costs of the electrolyser were expressed as the sum of a fixed term (function of the EL rated power) and a variable term (function of the electrical energy consumed by the electrolyser over the year) (Tractebel, 2017). It was assumed that the electrolyser operates at a pressure of 30 bar, while 200 bar is the maximum pressure of the hydrogen storage tank. A compressor is therefore required to pressurise hydrogen up to the hydrogen tank

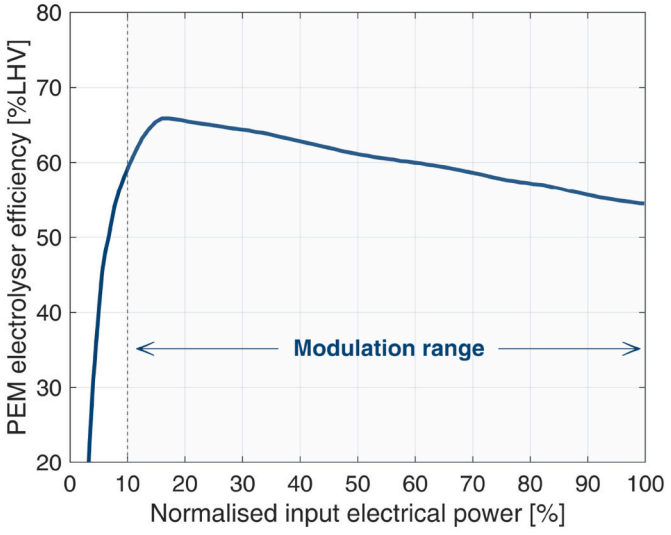

Fig. 4. Efficiency of the PEM electrolyser as a function of the input electrical power normalised with respect to the rated power.

Table 2
Results for different values of hydrogen share (HS).

Hydrogen share [%]	Electrolyser size [MW]	Compressor size [kW]	H_2 storage size [t]	$LCOE_t$ [€/kWh]	LCOH [€/kg]
0	0	0	0	0.10	–
10	8	0	0	0.12	10.54
20	16	0	0	0.14	10.56
30	25	0	0	0.17	10.57
40	34	0	0	0.19	10.58
50	43	0	0	0.21	10.60
60	52	0	0	0.23	10.61
70	62	0	0	0.26	10.64
80	74	37	0.3	0.28	10.67
90	87	144	1.7	0.31	10.71
100	97	298	14.7	0.33	10.83

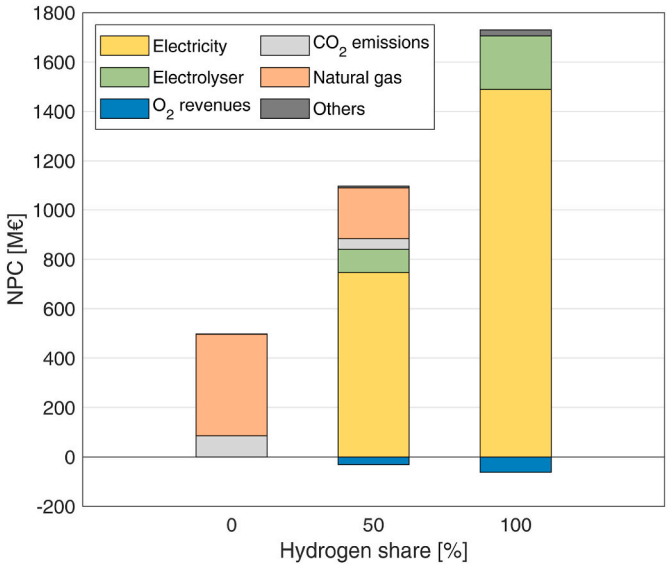

Fig. 5. NPC breakdown for different values of hydrogen share. The "Others" term includes the following contributions: costs of water, burners OPEX, H_2 compression, and H_2 tank.

pressure. Specifically, a three-stage intercooled compressor was considered, resulting in a specific consumption of 4 MJ/kg_{H2} when hydrogen is compressed from 30 bar (i.e., the operating pressure of the electrolyser) to 200 bar (Crespi et al., 2021). The specific investment cost for the hydrogen compressor was set to 1600 €/kW (Crespi et al., 2021). A specific CAPEX of 470 €/kg was assumed for the hydrogen storage (Tractebel, 2017), which is in line with the cost data of hydrogen tanks with an operating pressure of less than 250 bar (Danish Energy Agency, 2020).

As far as the furnaces are concerned, the analysis considers the operating costs as a function of the initial investment (3% of the CAPEX) (Loh et al., 2002). The investment cost for the furnaces was not taken into account in the NPC assessment, as they are already installed in the steel plant. In the case of conversion from natural gas to hydrogen, some redesign of the gas burner might be required, especially at high blending rates (IRENA, 2022). The conversion cost for MW-size industrial furnaces has been examined in (Durusut et al., 2019) and accounts for about 40% of the CAPEX of the furnaces. When applied to the steel plant case study, the conversion cost would always represent less than 0.5% of the NPC in the analysed scenarios. For this reason, this cost was not included in the cost assessment of this analysis.

The energy (electricity and natural gas) and carbon prices of the steel plant in 2021 are referred to as Reference scenario and they are shown in Table 1. The table also gives the prices of water and oxygen (Christensen, 2020; Morgenthaler et al., 2020): water is needed to feed the electrolyser, while oxygen was considered as a revenue, since it can be exploited on-site in the steel production process. The electricity and natural gas prices were taken as average values for industrial users in Italy in 2021 (Gestore dei Mercati Energetici SpA, 2022). The carbon price for the Reference scenario corresponds to the average value in the ETS market at the end of 2021 (Trading Economics, 2022). It is worth noting that the carbon price refers only to the direct CO_2 emissions of the plant (first term in Eq. (25)). All these prices were considered constant throughout the simulation period.

5. Results and discussion

The optimisation model was first applied to the Reference scenario, i.e. a scenario with current electricity and natural gas prices (0.18 and 0.08 €/kWh, respectively) and with a carbon price of 85 €/t. The optimal solution is to supply the furnaces with natural gas only, without the use

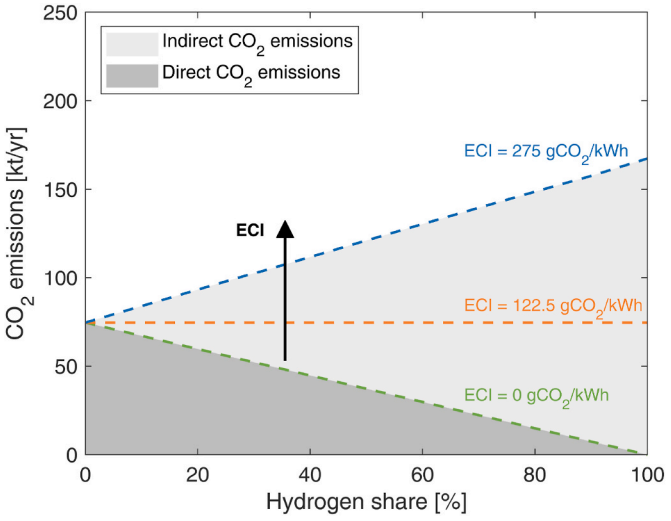

Fig. 7. Annual CO_2 emissions (direct and indirect) as function of hydrogen share and electricity carbon intensity (ECI). The green line represents a scenario with ECI equal to zero, i.e. there are no indirect emissions (locally available RES or grid supply with GO). The orange line represents a scenario where the ECI generates the same total emissions as the full-NG scenario. The blue line corresponds to a scenario with the EU average ECI for 2021.

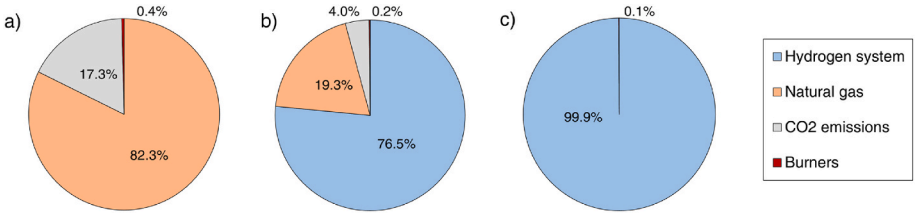

Fig. 6. NPC contributions for different values of hydrogen share: a) 0% (full-NG scenario), b) 50%, c) 100% (full-H_2 scenario). The "Hydrogen system" term includes the following contributions: electrolyser, H_2 compression, H_2 tank, electricity consumption, water consumption, and O_2 revenues.

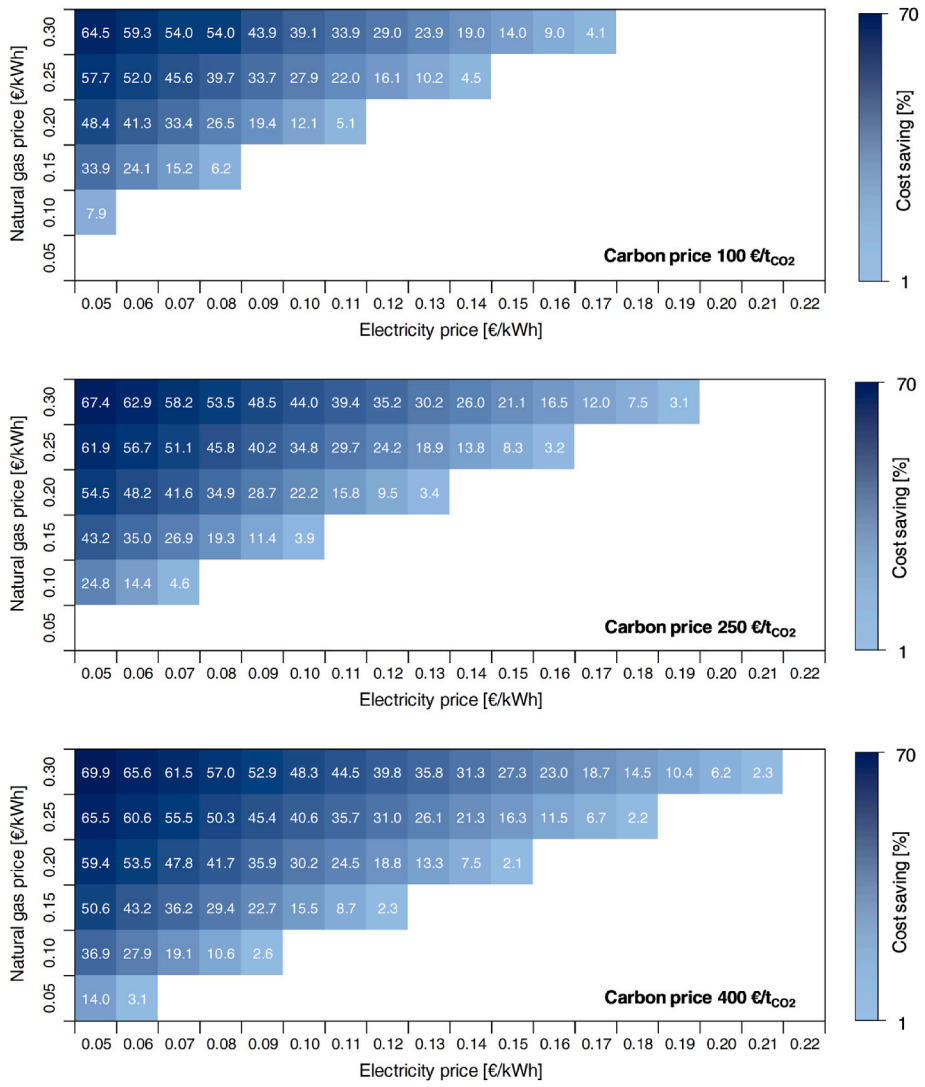

Fig. 8. Cost saving (CS) at variable carbon, electricity and natural gas prices. The white area corresponds to combinations of energy prices where hydrogen is not included in the optimal design of the energy system. In the white area the CS is null since the optimal solution is the NG-based configuration.

of hydrogen, resulting in a levelised cost of thermal energy ($LCOE_t$) of 0.10 €/kWh. The first row of Table 2 reports the main results for the Reference scenario (i.e. full-NG scenario).

A sensitivity analysis was then performed on the fraction of process heat demand covered by hydrogen (i.e. the hydrogen share was set as a constraint). The aim was to investigate the impact of hydrogen from an economic and environmental perspective. As shown in Table 2, the annual share of hydrogen was varied from 0% (Reference scenario) to 100% (full-hydrogen scenario). When the hydrogen share (HS) is increased, the size of the electrolyser increases, from 8 MW at 10% HS to 97 MW at 100% HS. It is worth noting that the hydrogen compressor and storage tank are not included in the energy system until the hydrogen share exceeds 80%. The size of the hydrogen storage is kept very small up to a hydrogen share of 90%, reaching 14.7 tonnes only in the full-hydrogen scenario. In scenarios with a high H_2 penetration, the hydrogen storage indeed becomes effective to avoid oversizing the electrolyser. On the other hand, if the hydrogen share is below 80%, the peaks of the thermal load are covered with natural gas and the electrolyser can meet the base load without the need for a storage system. This is possible because the HS constraint was defined on an annual basis, while the hourly gas composition at the burner inlet (i.e. hydrogen content) is a result of the optimisation model. However, in configurations where the hydrogen tank is not included in the optimal solution, an auxiliary H_2 energy buffer might be required to ensure a continuous hydrogen supply in case of maintenance or failure of the electrolyser system.

As shown in Table 2, the use of hydrogen at current energy prices leads to an increase in the $LCOE_t$ value, which changes linearly from 0.10 to 0.33 €/kWh (+230%) when moving from the Reference to the full-hydrogen scenario. The LCOH value increases slightly with increasing hydrogen share, in the range of 10.5–11 €/kg. This is mainly due to a decrease in the load factor of the electrolyser (from 53% at 10% HS to 44% at 100% HS). The use of hydrogen also leads to a reduction in the direct CO_2 emissions from 75 to 0 kt/yr, with a consequent reduction in the cost of CO_2 emissions.

Fig. 5 shows the breakdown of the NPC in three selected HS scenarios: 0% (Reference Scenario), 50% and 100%. The main NPC contributions for different values of hydrogen share are also displayed in Fig. 6, where the "Hydrogen system" term includes the costs due to electrolyser, H_2 compression, H_2 storage tank, electricity consumption, water consumption, and O_2 revenues.

The Reference scenario shows the lowest NPC (499 M€). The main contributions are the cost of natural gas purchased from the grid (82.3%) and the CO_2 emissions (17.3%), while the OPEX of the burners can be considered negligible. As the hydrogen share increases, the costs associated with the electrolyser, and especially the electricity purchased

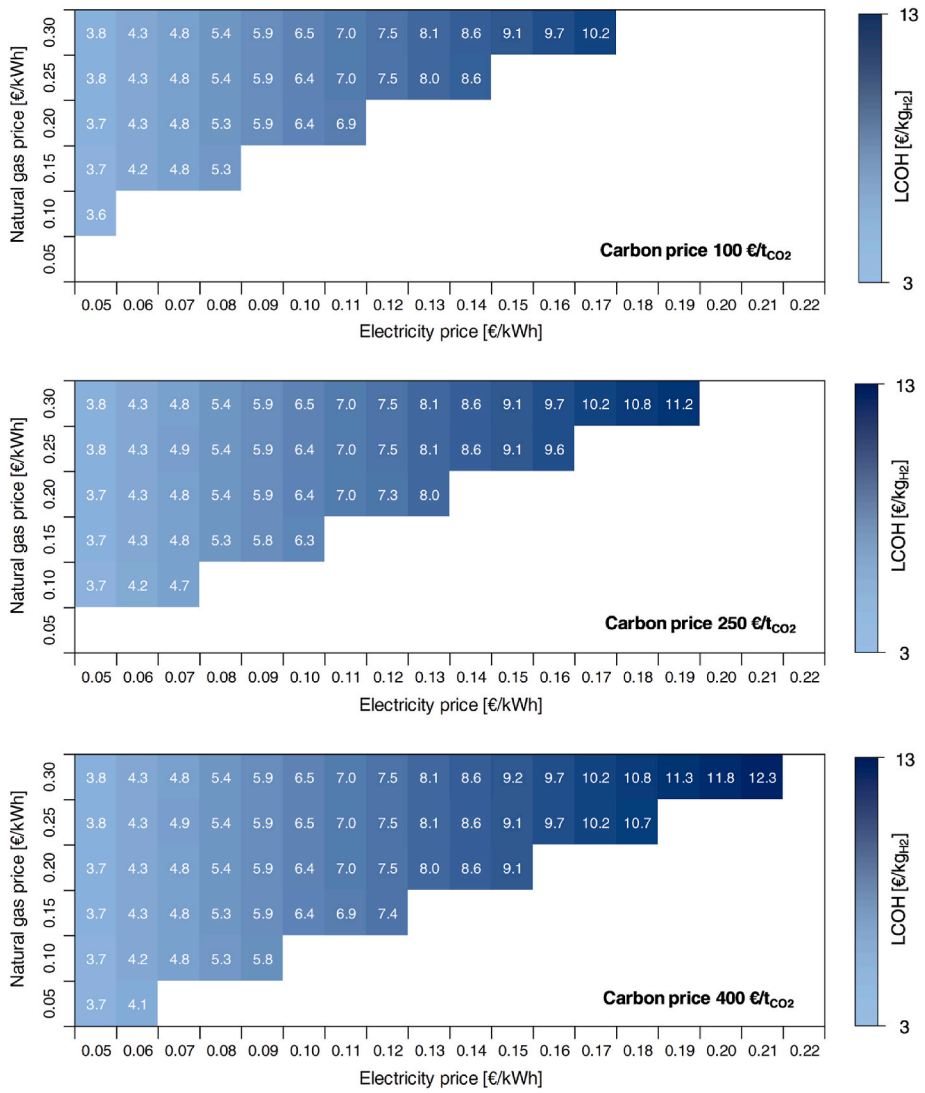

Fig. 9. Levelised cost of hydrogen (LCOH) at variable carbon, electricity and natural gas prices. The white area corresponds to combinations of energy prices where hydrogen is not included in the optimal design of the energy system.

from the grid, increase significantly. The NPC of the 50% HS scenario is 1066 M€ (+114% compared to the NG-fuelled scenario). The hydrogen system accounts for 76.5% of the NPC (mainly due to electricity and electrolyser contributions), while the shares of natural gas and CO_2 emissions drop to 19.3% and 4.0%, respectively. The production of hydrogen also generates oxygen as a by-product, that can be employed directly in the steel process. In this scenario, 30.8 M€ can be saved thanks to oxygen recovery, which corresponds to about 3% of the NPC. Moving to the full-hydrogen scenario (100% HS), the NPC increases to 1669 M€: almost all costs are due to the hydrogen system and there are no costs for natural gas and CO_2 emissions.

In order to better investigate the environmental impact (in terms of CO_2 emissions) of the proposed energy system, a sensitivity analysis on the electricity carbon intensity (ECI) was carried out, as shown in Fig. 7. Indeed, as reported in Eq. (25), total CO_2 emissions are composed of a direct term related to the use of NG from the grid and an indirect term depending on the electricity purchased and the ECI value.

Direct CO_2 emissions (dark grey area) decrease as the HS value is increased. In contrast, with increasing HS, an increase in indirect CO_2 emissions (light grey area) can be observed, the extent of which depends on the ECI value. The green dashed line in Fig. 7 corresponds to a scenario where the ECI value is zero, which can occur when using locally available renewable energy sources (RES) or electricity from the grid with guarantees of origin (GO). Electricity from the grid with GO is currently purchased by the steel plant analysed in this work. The blue dashed line was derived considering the EU average ECI for 2021 (275 g_{CO2}/kWh). As can be seen from the graph, when the ECI value is 275 g_{CO2}/kWh, the total CO_2 emissions are higher than those of the full-NG scenario (75 kt/yr) and reach a value of 167 kt/yr when the HS is 100%. The ECI value at which the total CO_2 emissions of the hydrogen-based scenario are equal to those of the full-NG scenario is about 123 g_{CO2}/kWh (lower values have already been reached in Sweden, France, Luxembourg, Lithuania, Finland, Austria and Slovakia).

To sum up, the use of hydrogen is always effective in reducing direct CO_2 emissions. However, an ECI value of less than about 123 g_{CO2}/kWh is required for hydrogen to become environmentally beneficial when considering total CO_2 emissions (i.e. sum of direct and indirect contributions).

To better understand the impact of the energy context on the economic profitability of hydrogen, a sensitivity analysis was conducted on the price of electricity and natural gas. The NG price was explored in the range of 0.05–0.30 €/kWh. Three different values of the carbon price were also examined: 100, 250 and 400 €/t. In this assessment, the optimisation framework evaluates when hydrogen is included in the optimal solution and provides the resulting values of hydrogen share (HS), levelized cost of hydrogen (LCOH) and cost saving (CS).

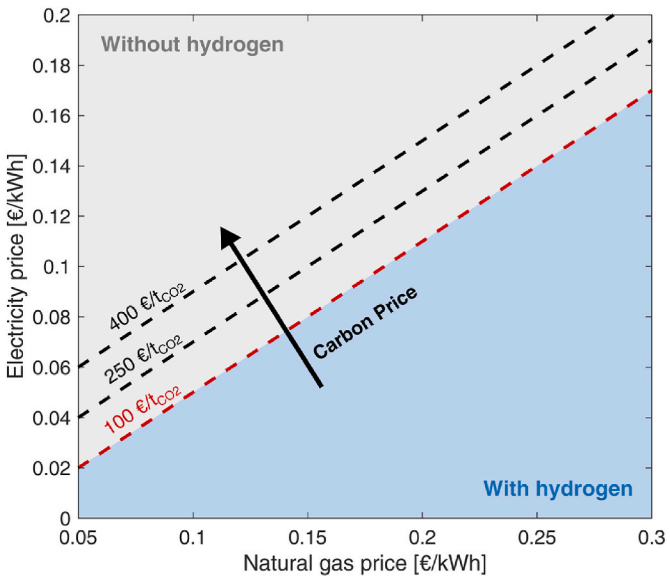

Fig. 10. Hydrogen convenience in the energy system as a function of the electricity and natural gas prices and for different values of carbon price (100, 250 and 400 €/t_{CO2}).

Table 3
Coefficients of the equation for the estimation of the economic profitability of hydrogen.

Coefficient	Value
a_1	0.6
a_2	$1.33 \cdot 10^{-4}$
a_3	$6.67 \cdot 10^{-3}$

The results are displayed in Fig. 8 and Fig. 9 for the CS and LCOH parameters, respectively. In these figures, the white area refers to the combinations of electricity and natural gas prices for which hydrogen is not included in the optimal design of the energy system. In contrast, the blue area corresponds to the hydrogen-based configurations, and the corresponding values of CS and LCOH are reported.

As can be seen in Fig. 8, hydrogen-based solutions can provide a cost saving in the range 2–70% compared to the full-NG scenario, depending on the energy and carbon prices. The hydrogen profitability, expressed by the CS indicator, improves by decreasing the electricity price and increasing the natural gas price. This means that the blue area tends to concentrate in the top left of the heatmaps, where the highest CS values can be observed. At a carbon price of 100 €/t, the cost saving is up to 64.5%, which is the case for electricity and gas prices of 0.05 and 0.3 €/kWh, respectively (top left corner of the heatmap). Moreover, an increase in the carbon price increases the number of energy price combinations for which hydrogen is economically beneficial. The blue area indeed expands when the carbon price varies from 100 to 400 €/t. For a given combination of energy prices, a higher carbon price leads to a higher CS: as an example, the highest CS value increases from 64.5% at 100 €/t to 69.9% at 400 €/t.

It is also worth noting that, when hydrogen starts to be advantageous from an economic point of view (i.e. transition from the white to the blue area), the annual hydrogen share in the optimal solution increases sharply, from zero to very high values, exceeding 80–90% in almost all scenarios (as shown in the HS heatmaps available in the Supplementary Material).

Fig. 9 shows the LCOH as a function of the energy and carbon prices. At a given gas price, the LCOH value increases with the price of electricity up to a certain threshold after which hydrogen is no longer included in the optimal design (white area). LCOH values up to 10–12 €/kg (depending on the carbon price) are achieved with electricity prices above 0.17 €/kWh. On the other hand, in scenarios with low electricity prices (i.e. 0.05–0.10 €/kWh), the cost of hydrogen drop to values in the range of about 3.6–6.5 €/kg. Low electricity prices may be representative of on-site electricity generation from local renewables (e.g. hydropower, photovoltaic or wind). As an example, a hydroelectric plant is available close to the steel plant, which could supply electricity at a price of about 0.06 €/kWh. Furthermore, the optimal LCOH values found in the low-electricity-price region are consistent with those found in the literature for the use of hydrogen as a decarbonisation vector in the steel industry (Kurrer, 2020; Wang et al., 2021; Vogl et al., 2018).

Based on the sensitivity analyses, a cost-optimal map of the economic suitability of hydrogen under variable energy and carbon prices was developed. Fig. 10 shows the electricity price below which hydrogen becomes economically convenient (dashed lines) for various natural gas and carbon prices. For example, at a natural gas price of 0.10 €/kWh and a carbon price of 100 €/t, the electricity price must be below 0.05 €/kWh to ensure a cost-effective use of hydrogen in the steel plant. If the carbon price rises to 400 €/t, an electricity price of about 0.09 €/kWh would be sufficient to have hydrogen as the optimal solution to cover the thermal demand. Thus, the blue area represents the combinations of electricity and natural gas prices for which hydrogen is included in the optimal energy system design (with a very high annual hydrogen share, as shown in the Supplementary Material). The grey area, on the other hand, represents energy prices for which hydrogen is not yet suitable and the optimal solution is to use only natural gas. To sum up, at a carbon price of 100 €/t, hydrogen becomes cost-effective if the electricity price is less than about 0.4–0.6 times the natural gas price. This value increases to 0.7–1.2 at a carbon price of 400 €/t.

Finally, based on Fig. 10, a general relationship was derived to define the electricity price below which hydrogen starts to be economically advantageous for a given gas price and carbon price. It is expressed by the following equation:

$$c_{el} = a_1 \cdot (c_{gas} - 0.05) + a_2 \cdot c_{CO_2} + a_3 \quad (27)$$

where c_{el} (in €/kWh) is the electricity price, c_{gas} (in €/kWh) is the gas price, c_{CO_2} (in €/t) is the carbon price, and a_1, a_2, and a_3 are the coefficients of the above relationship (shown in Table 3).

6. Conclusions

This work aims to assess the role of hydrogen as a fuel for the decarbonisation of heat generation in the steel sector. An MILP-based optimisation framework was developed to evaluate the optimal system configuration to cover the thermal demand of a steel plant. The model was then applied to a scrap-based EAF steel plant located in North Italy. The energy (electricity and natural gas) and carbon prices were varied to investigate their impact on the economic profitability of hydrogen. A cost-optimal map was finally derived to show the combination of electricity, natural gas and carbon prices that make hydrogen economically convenient. Main conclusions are summarised as follows:

- Hydrogen is always effective in reducing the direct CO_2 emissions of the steel plant. When total CO_2 emissions (direct + indirect) are taken into account, the electricity carbon intensity should be less than about 123 g_{CO2}/kWh for hydrogen to be environmentally profitable.
- The cost-effectiveness of hydrogen improves when the price of natural gas increases and the price of electricity decreases. At low electricity prices, the hydrogen-based configuration can result in cost savings of up to 60–70% compared to a full-NG scenario.
- LCOH values of less than about 6 €/kg can be obtained if the electricity price falls below 0.10 €/kWh, which could be achieved, for example, by generating electricity from on-site renewables.

- Hydrogen-based scenarios always involve a high value of hydrogen share, above 80–90% in all configurations. This means that, from a cost-optimal point of view, there is no gradual conversion to hydrogen. The optimal solution indeed involves a sharp transition to hydrogen when the energy context is favourable.
- As shown in the cost-optimal map (gas price in the range 0.05–0.3 €/kWh), at a carbon price of 100 €/t, hydrogen becomes advantageous if the electricity price is less than about 0.4–0.6 times the natural gas price. This value increases to 0.7–1.2 at a carbon price of 400 €/t.

Future studies will examine the effectiveness of using hydrogen as a reducing agent within the innovative DRI-EAF route. This is necessary, along with hydrogen-based heat supply (evaluated in this work), to move towards a deep decarbonisation of the steel sector.

CRediT authorship contribution statement

Paolo Marocco: Conceptualization, Methodology, Software, Formal analysis, Visualization, Investigation, Data curation, Supervision, Writing – original draft, Writing – review & editing. **Marta Gandiglio:** Conceptualization, Formal analysis, Visualization, Investigation, Data curation, Supervision, Writing – original draft, Writing – review & editing. **Davide Audisio:** Conceptualization, Software, Formal analysis, Investigation, Data curation, Writing – original draft. **Massimo Santarelli:** Supervision, Project administration, Funding acquisition.

Declaration of competing interest

The authors declare that they have no known competing financial interests or personal relationships that could have appeared to influence the work reported in this paper.

Data availability

Data will be made available on request.

Acknowledgments

The authors would like to thank Cogne Acciai Speciali SpA (Vincenzo Morreale, Energy Manager and Matteo Diani, Maintenance & Investments Director) and Blu Energie srl (Federico Oriani, Mattia Ogliengo and Michel Vuillermoz) for their support, provision of data and discussion on the present work.

Acronyms

BF	Blast furnace
BOP	Balance of plant
BOF	Basic oxygen furnace
CAPEX	Capital expenditures
CP	Compressor
CS	Cost saving
DRI	Direct reduced iron
EAF	Electric arc furnace
ECI	Electricity carbon intensity
EL	Electrolyser
ETS	Emissions trading system
GB	Gas burner
GO	Guarantee of origin
HS	Hydrogen share
HT	Hydrogen tank
$LCOE_t$	Levelised cost of (thermal) energy
LCOH	Levelised cost of hydrogen
LHV	Lower heating value
LOH	Level of hydrogen
MILP	Mixed integer linear programming
NG	Natural gas
OPEX	Operating expenditures
PEM	Proton exchange membrane
PWA	Piecewise affine
RES	Renewable energy sources

Supplementary Material

Supplementary Material to this article can be found online at https://doi.org/10.1016/j.jclepro.2023.135969.

References

Ampah, J.D., Jin, C., Rizwanul Fattah, I.M., Appiah-Otoo, I., Afrane, S., Geng, Z., Yusuf, A.A., Li, T., Mahlia, T.M.I., Liu, H., 2022. Investigating the evolutionary trends and key enablers of hydrogen production technologies: a patent-life cycle and econometric analysis, Int. J. Hydrogen Energy. https://doi.org/10.1016/J.IJHYDENE.2022.07.258.

Böhm, H., Zauner, A., Rosenfeld, D.C., Tichler, R., 2020. Projecting cost development for future large-scale power-to-gas implementations by scaling effects. Appl. Energy 264, 114780. https://doi.org/10.1016/J.APENERGY.2020.114780.

Christensen, A., 2020. Assessment of hydrogen production costs from electrolysis: United States and Europe. https://theicct.org/publication/assessment-of-hydrogen-production-costs-from-electrolysis-united-states-and-europe/.

Crespi, E., Colbertaldo, P., Guandalini, G., Campanari, S., 2021. Design of hybrid power-to-power systems for continuous clean PV-based energy supply. Int. J. Hydrogen Energy 46, 13691–13708. https://doi.org/10.1016/j.ijhydene.2020.09.152.

Danish Energy Agency, 2020. Energinet, technology data - energy storage. https://ens.dk/en/our-services/projections-and-models/technology-data.

Durusut, E., Mattos, A., Simon, R., Moore, I., Kiely, C., Yousif, S., Morris, S., Giles, A., 2019. Conversion of industrial heating equipment to hydrogen (WP6 final report, Hy4Heat project). https://www.hy4heat.info/reports.

E&M Combustion, 2020. Hydrogen combustion systems for the decarbonization of the industry. Spain. https://emcombustion.es/wp-content/pdfs/en/EM&C_hydrogen_burners.pdf.

EUROFER (European Steel Association), 2022. Annual report 2022. Brussels. https://www.eurofer.eu/assets/publications/reports-or-studies/annual-report-2022/EUROFER-Annual-Report-2022.pdf.

Fan, Z., Friedmann, S.J., 2021. Low-carbon production of iron and steel: technology options, economic assessment, and policy. Joule 5, 829–862. https://doi.org/10.1016/J.JOULE.2021.02.018.

Gestore dei Mercati Energetici SpA, 2022. GME official website. https://www.mercatoelettrico.org/it/. (Accessed 12 September 2022).

Hoffmann, C., Van Hoey, M., Zeumer, B., 2020. Decarbonization challenge for steel - hydrogen as a solution in Europe. Luxembourg. https://www.mckinsey.com/industries/metals-and-mining/our-insights/decarbonization-challenge-for-steel.

IBM, 2022. IBM ILOG CPLEX optimization studio. https://www.ibm.com/products/ilog-cplex-optimization-studio. (Accessed 2 October 2022).

IEA, 2019. The future of hydrogen. Paris. https://www.iea.org/reports/the-future-of-hydrogen.

IEA, 2020. Iron and steel technology roadmap. Paris. https://www.iea.org/reports/iron-and-steel-technology-roadmap.

IEA, 2021. Global energy review 2021. Paris. https://www.iea.org/reports/global-energy-review-2021.

IRENA, 2022. Green hydrogen for industry: a guide to policy making. Abu Dhabi. https://www.irena.org/publications/2022/Mar/Green-Hydrogen-for-Industry.

Karakaya, E., Nuur, C., Assbring, L., 2018. Potential transitions in the iron and steel industry in Sweden: towards a hydrogen-based future? J. Clean. Prod. 195, 651–663. https://doi.org/10.1016/j.jclepro.2018.05.142.

Kurrer, C., 2020. The potential of hydrogen for decarbonising steel production. Brussels. https://www.europarl.europa.eu/thinktank/en/document/EPRS_BRI(2020)641552.

Leicher, J., Nowakowski, T., Giese, A., Görner, K., 2018. Hydrogen in natural gas: how does it affect industrial end users?. In: World Gas Conf Washington DC.

Liu, W., Zuo, H., Wang, J., Xue, Q., Ren, B., Yang, F., 2021. The production and application of hydrogen in steel industry. Int. J. Hydrogen Energy 46, 10548–10569. https://doi.org/10.1016/J.IJHYDENE.2020.12.123.

Loh, H.P., Lyons, J., White, C.W., 2002. Process equipment cost estimation final report. https://www.osti.gov/servlets/purl/797810.

Marocco, P., Ferrero, D., Martelli, E., Santarelli, M., Lanzini, A., 2021a. An MILP approach for the optimal design of renewable battery-hydrogen energy systems for off-grid insular communities. Energy Convers. Manag. 245, 114564 https://doi.org/10.1016/j.enconman.2021.114564.

Marocco, P., Ferrero, D., Lanzini, A., Santarelli, M., 2021b. Optimal design of stand-alone solutions based on RES + hydrogen storage feeding off-grid communities. Energy Convers. Manag. 238, 114147 https://doi.org/10.1016/j.enconman.2021.114147.

Marocco, P., Gandiglio, M., Santarelli, M., 2022. When SOFC-based cogeneration systems become convenient? A cost-optimal analysis. Energy Rep. 8, 8709–8721. https://doi.org/10.1016/j.egyr.2022.06.015.

Mayrhofer, M., Koller, M., Seemann, P., Prieler, R., Hochenauer, C., 2021. Assessment of natural gas/hydrogen blends as an alternative fuel for industrial heat treatment

furnaces. Int. J. Hydrogen Energy 46, 21672–21686. https://doi.org/10.1016/j.ijhydene.2021.03.228.
Morgenthaler, S., Ball, C., Koj, J.C., Kuckshinrichs, W., Witthaut, D., 2020. Site-dependent levelized cost assessment for fully renewable Power-to-Methane systems. Energy Convers. Manag. 223, 113150 https://doi.org/10.1016/J.ENCONMAN.2020.113150.
Öhman, A., Karakaya, E., Urban, F., 2022. Enabling the transition to a fossil-free steel sector: the conditions for technology transfer for hydrogen-based steelmaking in Europe. Energy Res. Social Sci. 84 https://doi.org/10.1016/j.erss.2021.102384.
Proost, J., 2019. State-of-the art CAPEX data for water electrolysers, and their impact on renewable hydrogen price settings. Int. J. Hydrogen Energy 44, 4406–4413. https://doi.org/10.1016/j.ijhydene.2018.07.164.
Rechberger, K., Spanlang, A., Sasiain Conde, A., Wolfmeir, H., Harris, C., 2020. Green hydrogen-based direct reduction for low-carbon steelmaking. Steel Res. Int. 91, 2000110 https://doi.org/10.1002/SRIN.202000110.
Spreitzer, D., Schenk, J., 2019. Reduction of iron oxides with hydrogen—a review. Steel Res. Int. 90, 1900108 https://doi.org/10.1002/SRIN.201900108.
Tractebel, Hinicio, 2017. Study on early business cases for H2 in energy storage and more broadly power to H2 applications. https://www.clean-hydrogen.europa.eu/media/publications/study-early-business-cases-h2-energy-storage-and-more-broadly-power-h2-applications_en.
Trading Economics, 2022. EU carbon permits. https://tradingeconomics.com/commodity/carbon. (Accessed 12 September 2022).
Vogl, V., Åhman, M., Nilsson, L.J., 2018. Assessment of hydrogen direct reduction for fossil-free steelmaking. J. Clean. Prod. 203, 736–745. https://doi.org/10.1016/J.JCLEPRO.2018.08.279.
Wang, R.R., Zhao, Y.Q., Babich, A., Senk, D., Fan, X.Y., 2021. Hydrogen direct reduction (H-DR) in steel industry—an overview of challenges and opportunities. J. Clean. Prod. 329, 129797 https://doi.org/10.1016/j.jclepro.2021.129797.
Zauner, A., Böhm, H., Rosenfeld, D.C., Tichler, R., 2019. Innovative large-scale energy storage technologies and Power-to-Gas concepts after optimisation: analysis on future technology options and on techno-economic optimization (Deliverable 7.7, Store&Go EU Project). https://www.storeandgo.info/publications/deliverables/index.html.
Zhang, X., Jiao, K., Zhang, J., Guo, Z., 2021. A review on low carbon emissions projects of steel industry in the World. J. Clean. Prod. 306, 127259 https://doi.org/10.1016/J.JCLEPRO.2021.127259.